JOURNAL OF MATERIALS SCIENCE **35** (2000) 345–352

Titanium local environment and electrical conductivity of TiO_2-doped stabilized tetragonal zirconia

F. CAPEL, C. MOURE, P. DURÁN
Instituto de Cerámica y Vidrio (CSIC), Departamento de Electrocerámica, 28500-Arganda del Rey, Madrid, Spain

A. R. GONZÁLEZ-ELIPE, A. CABALLERO
Instituto de Ciencia de Materiales de Sevilla (CSIC-Univ. de Sevilla) y Dto. de Química Inorgánica, Centro de Investigaciones Científicas "Isla de la Cartuja," Avda. Américo Vespucio s/n, 41092 Sevilla, Spain

Solid state reactions in the ZrO_2-Y_2O_3-TiO_2 system have been studied and the solid solubility limit of TiO_2 in yttria stabilized tetragonal zirconia Y-TZP has been stablished. Structural characterization was carried out by XRD studies, and the changes in local structures with increasing TiO_2 in yttria stabilized tetragonal zirconia was analyzed for the first time by EXAFS and XANES measurements. The XANES results indicate a displacement of Ti ions from the center of symmetry with increasing titania content leading to assume a non randomly substitution of Ti^{4+} on Zr^{4+} sites in the tetragonal zirconia lattice. From the Ti-O and Ti-Ti measured distances, it has been assumed that the found electrical conductivity decrease with increasing titania content was due to both a trapping of the oxygen ion vacancies at Ti ions (Ti'_{Zr} Vö) and the formation of more complex associations like (Ti'_{Zr} Vö Ti'_{Zr} Vö), which giving rise to a reduction in the global concentration of moving oxygen vacancies.

1. Introduction

Ceramic oxides exhibiting both oxygen ion and electronic conductivity are commonly known as mixed-conductors and, as such, are attracting interest as candidates to be used as electrodes, mainly anodes, in several applications as for example in SOFC devices, oxygen separation membranes and electrocatalist for the partial oxidation hydrocarbons [1–3]. These mixed-conducting oxides can improve the charge-transfer in the electrode reaction area reducing, thus, the detrimental polarization losses found in the electrodes conventionally used, as for example Ni-zirconia or $La_{1-y}Sr_yMnO_{3-y}$, at the operating conditions of such devices [4].

At the last decade many efforts have been devoted to the study of the mixed-conducting YSZ by dissolving in its structure some metal-transition oxides and/or Ce_2O_3 [5], but the low solubility of the former and the strong temperature and oxygen partial-pressure electronic conductivity dependence of the later precludes their use as anode materials in SOFC devices. Recently the research efforts have been concentrated mainly on the TiO_2-stabilized cubic zirconia (TiO_2-YSZ), and several papers with contradictory results have been published [6–9]. In the same way, TiO_2-doped stabilized tetragonal zirconia (TiO_2-YTZP), as a pure oxygen ion conductor with a conductivity higher than TiO_2-YSZ below 700 °C, its electrical behavior have been the object of a few publications more recently [10, 11]. The true role of titania in decreasing or increasing the conductivity of YSZ and/or YTZP was not reported. For understanding physical properties such as diffusion and, mainly, the ionic conduction, it is the changes in local structure and short-range order with different dopant concentration that are most important [12]. Based on those results, the relationship between the Ti-local structure and conductivity of the TiO_2-YTZP sintered samples will be discussed. Determination of Ti-local environment was carried out by analysis of EXAFS, and the site symmetry of the Ti ions as well as the Ti ion valences in the tetragonal zirconia lattice by analysis of the XANES features. The a.c. complex impedance spectroscopy for the electrical conductivity measurements in air was used.

2. Experimental procedure

The samples of Y-TZP containing 5 to 20 mol % TiO_2 were prepared as detailed elsewhere [13]. Briefly, yttria-doped tetragonal zirconia, Y-TZP, powders (3 mol % Y_2O_3 from Tosoh Co.) with TiO_2 content ranging from 0 to 20 mol % were prepared by precipitating, on an aqueous suspension of the Y-TZP powders, the appropriate amount of titanium tetrabutoxide with ammonium hydroxide. The final pH of the suspension

was >9 to ensure a quantitative titanium hydroxide precipitation. A homogeneous powder of Y-YZP microspheres coated by the titanium hydroxide nanoparticles was obtained at the end of the precipitation process. After being dried at 120 °C overnight in air the powders were ball-milled in methanol for 2 h, redried at 80 °C for 5 h, and calcined at 900 °C for 2 h. After calcining the powders were ground and isopressed at 200 MPa and sintered at 1400 °C for 5 h in air. The sintering density of all the samples was higher than 96% of theoretical, and the grain size varied from 0.3 μm (undoped Y-TZP) to 2 μm (20TiO_2-Y-TZP). The crystal structures of the sintered samples were studied using X-ray diffractometer (Siemens D-5000), measuring the variation of the lattice parameters a and c with increasing titania content. The precision in the lattice parameter measurements was in the $\pm$0.0005 nm range.

X-ray absorption measurements at the Ti-K edge were made at the storage ring (DCI D44 station) at the LURE synchrotron in Orsay (France) under the operating conditions of 1.85 GeV electron energy and 250 mA ring current. Energy selection was accomplished by using a double crystal monochromator with Si (1 1 1) crystals.

In the specific case of the TiO_2-Y-TZP samples, the required amounts of TiO_2-YTZP powders were diluted with boron nitride powder and pressed into an aluminum sample cell with X-ray transparent windows. The XAS spectra were collected at liquid-nitrogen temperature in the transmission mode and using two gas ionization chambers as detectors. The XAS spectra were taken at the Ti-K absorption edge within the energy range between 4900 and 5700 eV with a step width of 0.5 eV. A Ti-foil standard (4964.5 eV) was used for energy calibration.

For analysis of the XANES region, the spectra were normalized as previously described in many published papers [14] avoiding, where it was possible, deviations between the data and tabulated X-ray absorption coefficients both below and above the edge.

Given that reliable quantitative XANES calculations have only been possible on solids with simple structures, the interpretation of geometrical and chemical changes in more complex structures, as is the present case of TiO_2-Y_2O_3-ZrO_2 solid solutions, will be limited to a qualitative study of these compounds and comparing them with other well known samples as a reference. On the other hand, the subsequent XAS studies were carried out only on those samples which appeared to contain the tetragonal zirconia solid solution as the only phase according to XRD. Thus the features of Ti-K XANES for TiO_2-YTZP fine powders containing 5 and 10 mol % TiO_2 were used as "fingerprints" to analyze the structural changes, if any, produced as a consequence of the solid solution of TiO_2 into yttria-doped tetragonal zirconia.

The EXAFS spectra were analyzed using the standard EXAFS plane wave equation:

$$\chi(k) = \sum_j \frac{N_j}{kR_j^2} F_j(k) \exp\left(-2\sigma_j^2 k^2\right) \exp\left(\frac{-2R_j}{\lambda}\right) \times \sin[2kR_j + \phi_j(k)] \quad (1)$$

where k is the momentum of the photoelectron ejected in the X-ray absorption process, and χ the normalized oscillations of the fine structure. All the structural parameters contained in that equation as well as their interdependence have been widely described in the literature [15, 16] and it will not be repeated again here. However, it must be mentioned that the EXAFS spectra were analyzed using the theoretical amplitude and phases shift function proposed by Rehr *et al.* [17]. In that way the coordination numbers (N_j), the bond distance (R), and the relative bond length disgregation or Debye-Walle factor ($\Delta\sigma^2$) with reference to the model compound were obtained. To take as an example in this study Fourier Transforms (FTs) of Ti EXAFS from $K = 2$ to 12 Å^{-1} were back-transformed from $R = 1$ to 2.1 Å to obtain the Ti-O first shell and $R = 2$ to 3 Å for the Ti-Ti second shell. These FTs give pseudo-radial distribution function around the absorber cations, and curve fitting, as mentioned above, utilized the theoretical amplitude and phase shift functions calculated from the FEFF program [17]. For Ti EXAFS, empirical amplitude and phase functions derived from TiO_2 were used to fit the Ti-O shells, with Fourier filter windows of 0.9–1.8 Å.

Platinum paste (Engelhard 6082) was painted on both sides of the sintered discs and dried in an oven at 120 °C to eliminate the solvent. After drying, the electrode samples were annealed at 800 °C for a short time, about 30 min, to avoid an excessive shrinkage of the platinum electrodes. To these electroded samples were welded platinum lead wires and placed in the hot zone of a programmed furnace with a chrome-alumel thermocouple located on the mid point of the electrode sample.

The temperature dependence of electrical conductivity measurements were carried out by using an Impedance Analyzer (Hewler Packard model 4192A) in the frequency range of 5 Hz to 13 MHz. Measurements were made in air in the temperature range of 200 to 800 °C. For comparison, an undoped Y-TZP sample sintered in the same conditions as for TiO_2-doped Y-TZP ones was used.

3. Experimental results

3.1. X-ray diffraction studies

As it can be seen in Fig. 1 the lattice parameters a and c of tetragonal zirconia Y-TZP decrease and increase respectively, with increasing TiO_2 concentration and appear to reach a constant value at about 13 mol % TiO_2. The same Fig. 1 shows the variation of the tetragonality c_t/a_t as a function of the TiO_2 content. As shown, the tetragonality remains constant beyond 12 mol % TiO_2, confirming the statement for the solubility limit for TiO_2 in tetragonal zirconia Y-TZP. These results are consistent with the SEM observations, not shown here, in which a composition containing 15 mol % TiO_2 showed a considerable amount of a second phase, the zirconium titanate (ZT), and an enhanced grain growth. Therefore, the solubility limit of TiO_2 into tetragonal zirconia Y-TZP is well bellow 15 mol % up to 1400 °C. These solid solubility data for TiO_2 in Y-TZP are consistent with that established (13 mol %) by mean of Raman spectroscopy elsewhere [18], and they are in

TABLE I Calculated Zr-O bond lengths as a function of titanium dioxide content

Composition (mol %)			Length (nm)	
ZrO_2	Y_2O_3	TiO_2	Zr-O_I	Zr-O_{II}
97[a]	3	—	0.2080	0.2380
97	3	—	0.2093	0.2355
92	3	5	0.2079	0.2371
87	3	10	0.2065	0.2380

[a]Ref. 22.

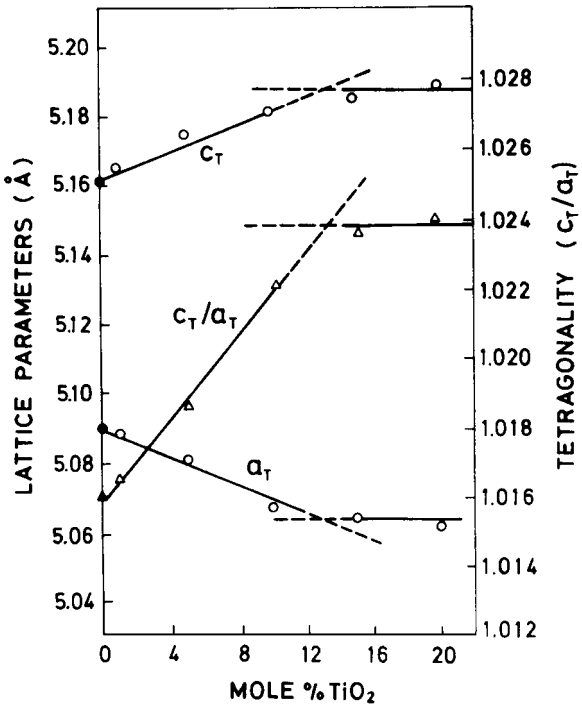

Figure 1 Variation of unit-cell dimensions and tetragonality c_t/a_t of TiO_2-doped Y-TZP solid solutions after sintering at 1400 °C.

close agreement with those of Hoffman *et al*. [19] and Rog and Borchardt [11].

The zirconia-oxygen bond lengths in Y-TZP can be easily estimated from the precision lattice parameters measurements [20]. The calculated values for Y-TZP and TiO_2-doped Y-TZP solid solutions are listed in Table I. The calculated bond lengths of Y-TZP are nearly the same to those measured for Zr-O_I and Zr-O_{II}, 0.208 and 0.238 nm, respectively, elsewhere [21]. A slight decrease or increase for Zr-O_I and Zr-O_{II} bond lengths respectively, in Y-TZP as a result of the increased TiO_2 content takes place. These results confirm the statement established elsewhere [18] by Raman spectroscopy that the local bonding environment of the tetravalent cations Ti^{4+} to O^{2-} in the ZrO_2-Y_2O_3-TiO_2 system is different from that of cations in the binary ZrO_2-Y_2O_3 one, where cations are eight-fold coordinated. On the other hand, given that the ionic radius of Ti^{4+} for sixfold coordination is 0.074 nm, it was argued that the found selective Raman shifts arised from the occupation of the tetravalent ions Ti^{4+} in distorted, presumably pentahedral, sites in the tetragonal zirconia crystal lattice [18].

3.2. EXAFS spectra at the Ti-K edge

The room temperature Ti K-edge EXAFS spectra of the two 5Ti-YTZP and 10Ti-YTZP tetragonal zirconia solid solutions are shown in Fig. 2a. As mentioned before, the energy zero was taken as the K-edge energy of pure Ti metal (4966.4 eV). The normalized Ti-EXAFS for those tetragonal zirconia solid solutions plotted as $x(k)$ are shown in Fig. 2b, and the Fourier transformation of these radial structure peak yields a filtered $\chi(k)$ signal, as shown in Fig. 2d, which were used to study the local structure around titanium cations.

Utilizing amplitude and phase shift function derived from the TiO_2 model system a quantitative analysis of the first Ti-O shell, as shown in Fig. 2c, was performed. The first mayor peak, between about 1.3 and 2 Å, in the FTs corresponds to the nearest neighbor around the Ti cation and the second peak, between 2 and 3 Å, corresponds to the next nearest neighbors, i.e. Ti-Ti or Ti-Zr cations. The peaks for higher R values belonging to outer cation-cation shell. From the FTs a slight decreasing of the amplitude of Ti-EXAFS with increasing TiO_2 content can be noticed, which is in close agreement with the obtained results for Ce-doped tetragonal zirconia [22], and indicates an increased distortion of the cation network.

Quantitative fitting results, as it is shown in Table II, for the Ti-O shell led to two sets of bond lengths 1.73 and 1.87 Å for the 5Ti-YTZP solid solution, and a total coordination number of ∼6. In the same way, also two sets of bond lengths 1.88 and 2.05 Å with a total coordination number of ∼4 were found for the 10Ti-YTZP solid solution. Thus, the local environment around Ti^{4+} seems to be concentration-dependent [23]. Therefore these results are consistent with a change of coordination number (6 to 5 or 4 for Ti) from pure TiO_2 to tetragonal zirconia solid solutions. Finally, quantitative fitting of the first Ti-cation (Zr and/or Ti) shell were performed using calculated amplitude and phase functions of a Ti-Ti pair. A distance of 2.81 Å was obtained in the specific case of the 10Ti-YTZP tetragonal zirconia solid solution. No quantitative analysis was performed for the 5Ti-YTZP one. That Ti-Ti distance is much shorter than that of the corresponding Zr-cation shell (3.61 to 3.62 Å) [24]. This can indicate that Ti^{4+} ions do not randomly substitute Zr^{4+} lattice sites according to a statistical process [25].

3.3. XANES spectra

X-ray absorption near-edge (XANES) spectra at the Ti-K absorption edge for 5Ti-YTZP and 10Ti-YTZP were shown in Fig. 2a. Given that the structure of both samples is tetragonal the spectra are quite similar. The

TABLE II Fitting results of Ti EXAFS for Ti-doped tetragonal zirconia samples

	M-O	R (Å)	CN	$\Delta\sigma^2$ (Å$^2 \times 10^3$)
First shell				
5Ti-YTZP	Ti-O	1.73	2.6	0.1
	Ti-O	1.87	3.8	0.1
10Ti-YTZP	Ti-O	1.88	2.2	0.1
	Ti-O	2.05	1.6	0.1
Second shell				
10Ti-YTZP	Ti-Ti	2.81	2.2	0.1

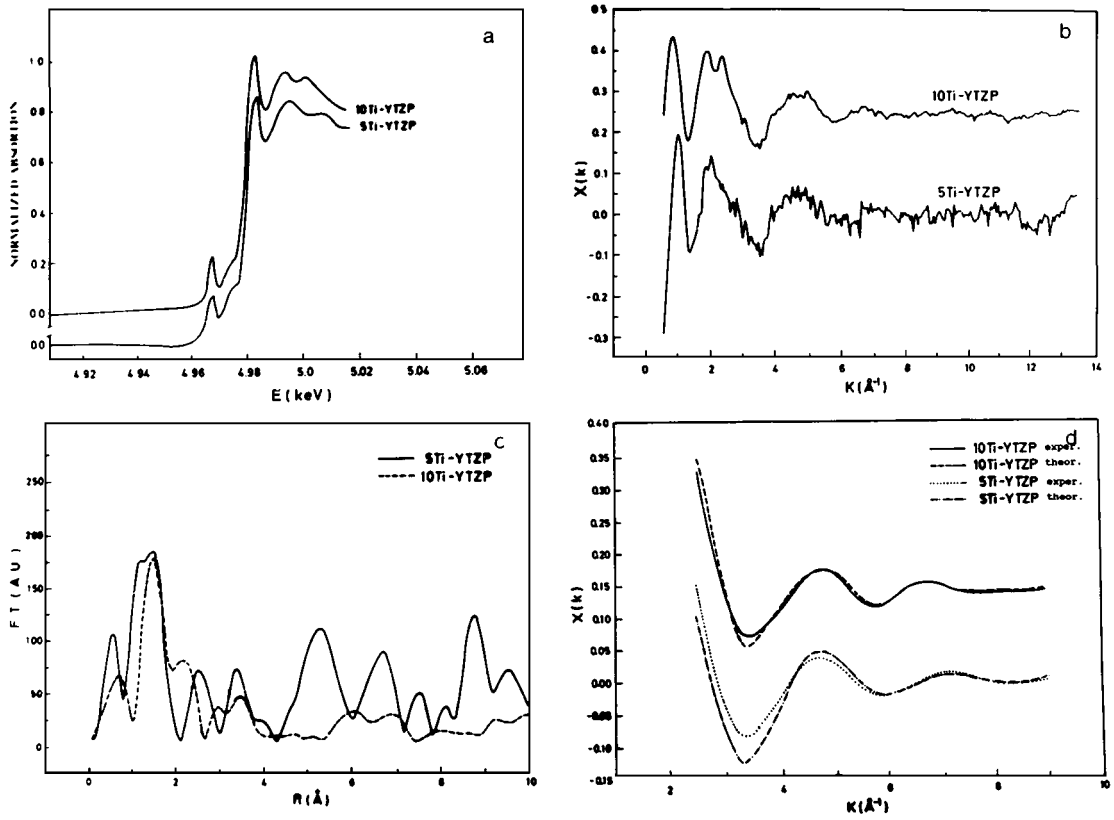

Figure 2 X-ray absorption of 5Ti-YTZP and 10Ti-YTZP tetragonal zirconia solid solutions at the Ti-K edge, XANES (a), Normalized EXAFS $\chi(k)$ (b), Fourier transform (c), and Inverse transform of (c) in (d).

energy of the Ti-K absorption edge corresponds to the electronic transition from the 1s core level to unoccupied high-energy states, and has been determined as the inflexion point of rising edge of the XAS data. Such a shoulder was located at about 4972.8 eV which is somewhat higher than that of metallic Ti as consequence of the different oxidation state of that cation in both cases. For energies lower than that of the Ti-K absorption edge a relatively sharp pre-peak located at almost the same energy (4967.5 eV) but with different intensity for 5Ti-YTZP and 10Ti-YTZP samples, was present in the XANES spectra. Above the Ti-K absorption edge the XANES spectra display a prominent peak located at slightly different energies, 4983.6 and 4983.2 eV, for 5Ti-YTZP and 10Ti-YTZP samples respectively.

Given that the XANES spectra can be taken as the finger-prints to be compared with those of the well-know structure compounds as reference, then the XANES spectra of our tetragonal zirconia solid solutions were compared with those, of the rutile (with Ti ions six-fold coordinated), $Ti(OEt)_4$ (five-fold coordinated), and Ba_2TiO_4 and $Ti(OAm)_4$ (four-fold coordinated), respectively [26–29] as shown in Fig. 3. The octahedral coordinated compounds (rutile and/or anatase) are characterized by several pre-edge peaks of low intensity and centered at an energy of 4968 eV, Ba_2TiO_4 and Ti-$(OAm)_4$ with Ti ions tetrahedral coordinated exhibited a strong pre-edge peak at an energy of 4967 eV, and $Ti(OEt)_4$ with Ti ions coordinated by five oxygen ions in a square-pyramidal distribution showed a relatively sharp pre-edge peak at 4967.5 eV. Then, from the above XANES spectra data it seems reasonable to state that the intensity, shape and energy position (4967.5 eV) of the pre-edge peak of the Ti-YTZP tetragonal zirconia solid solutions compares well with that of the $Ti(OEt)_4$ compounds with a square-pyramidal arrangement.

The characteristics of the post-edge peak present in the Ti-YTZP XANES spectra, i.e. lower energy and higher intensity for increasing TiO_2 content, can indicate a change in the geometrical arrangement of the scattered ions in the Ti environment. Such a suggestion is consistent with the results of Zschech *et al.* [25].

The Mg K_α XP spectrum for the Ti-(2p) core level showed two peaks at binding energies of 458.5 and 464.2 eV which corresponding to Ti $2p_{3/2}$ and $2p_{1/2}$, respectively, for Ti^{4+}. Peaks for Ti^{3+}, if any, should appear at energies of 457.2 and 463.0 eV. Therefore, no evidence for the presence of reduced Ti^{3+} was found from the XPS results on 10Ti-Y-TZP sample sintered at 1400 °C.

3.4. Total electrical conductivity in air

The ac conductivity results were plotted in the complex impedance plane, and as an example typical ac impedance spectrum for titania-doped tetragonal zirconia (5Ti-YTZP) at 449 °C is shown in Fig. 4. As it can be seen, three well developed semicircles can be distinguished which are related to the bulk, grain boundary, and electrode relaxation phenomena at high, intermediate, and low frequencies respectively [30]. From the intersection of the first semicircle at the lower frequency with the real axis the bulk resistance can be obtained. In the same way the sum of bulk and grain boundary

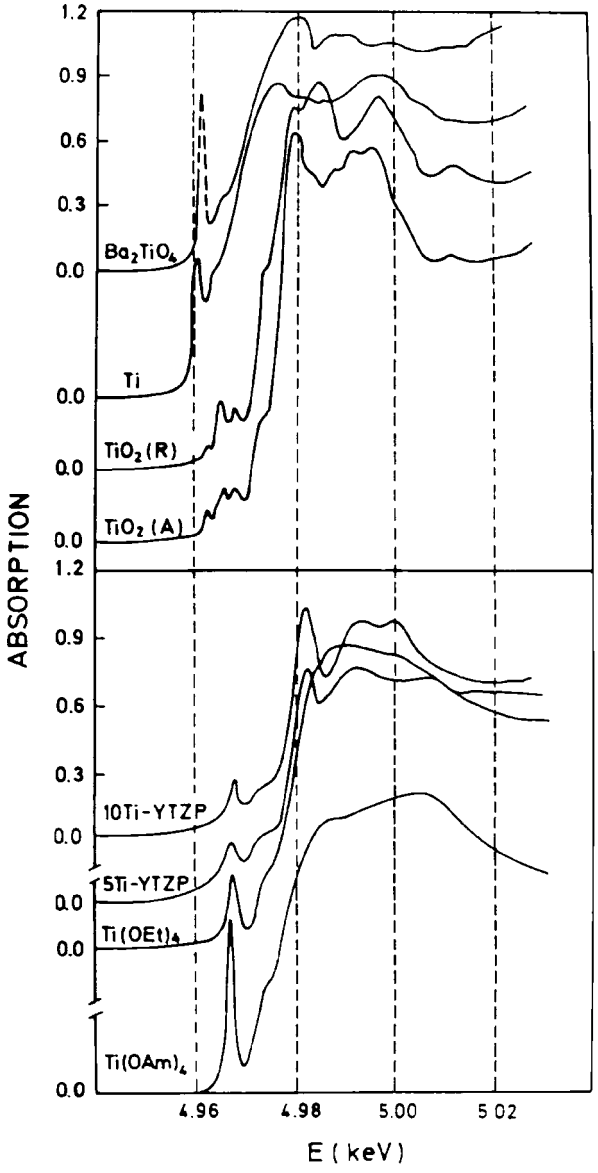

Figure 3 Comparison plot of K-edge XANES spectra of Ti in 5Ti-YTZP and 10Ti-YTZP tetragonal zirconia solid solutions with several Ti-O reference compounds.

resistances was calculated from the second one. From the intersection of the third one, the sum of bulk, grain boundary and electrode resistances can be estimated. The specific total conductivity (σ_t) can be easily calculated taking into account the platinum electrode area (A) on either side of the sample, and the length (L) between the two platinum electrodes. For example, the bulk conductivity (σ_b) was calculated using the following known equation [31]:

$$\sigma_b = \frac{1}{R_b}\frac{L}{A} \tag{2}$$

where R_b is the intersection of the first semicircle as indicated in Fig. 4. A quite similar ac impedance spectrum was obtained for the 10Ti-YTZP sample. It must be mentioned that poorly developed grain boundary semicircles were obtained with increasing temperature in both titania-doped YTZP samples, and it become difficult to analyze the impedance data in terms of bulk and grain boundary contributions. However, in order to know what is the predominant conduction mechanism, an attempt to calculate the bulk and grain boundary conductivities at that temperature range in which the two first semicircles were quite well developed, was made. With these conductivity data and assuming that the electrical conductivity σ follows an Arrhenius equation of the type:

$$\sigma = \sigma_o \exp(-E_a/RT) \tag{3}$$

where T is the absolute temperature, σ_o is a constant, E_a is the activation energy for the motion of charges, and R is the gas constant, the temperature dependence of the bulk, grain boundary, and total conductivities for 5Ti-YTZP, 10Ti-YTZP, and undoped Y-TZP samples was studied. In Table III the activation energy values for the three samples in the temperature range of 300 to 700 °C are shown.

From the Arrhenius plot a general trend to decrease the electrical conductivity with increasing titania

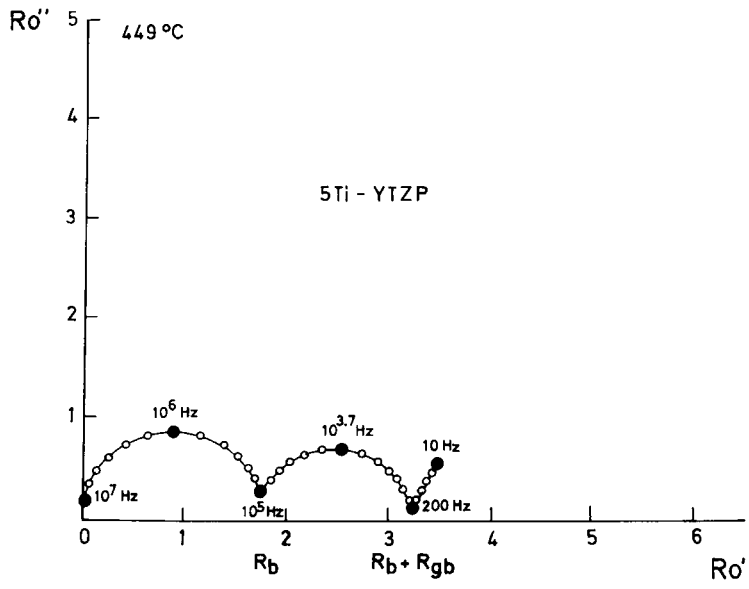

Figure 4 Complex impedance plots for 5Ti-YTZP at 449 °C in air.

TABLE III Activation energy values (eV) of the conductivity

Sample	σ_b	σ_{gb}	σ_t
YTZP	0.86	1.01	0.90
5Ti-YTZP	0.97	1.17	1.04
10Ti-YTZP	1.02	1.16	1.04

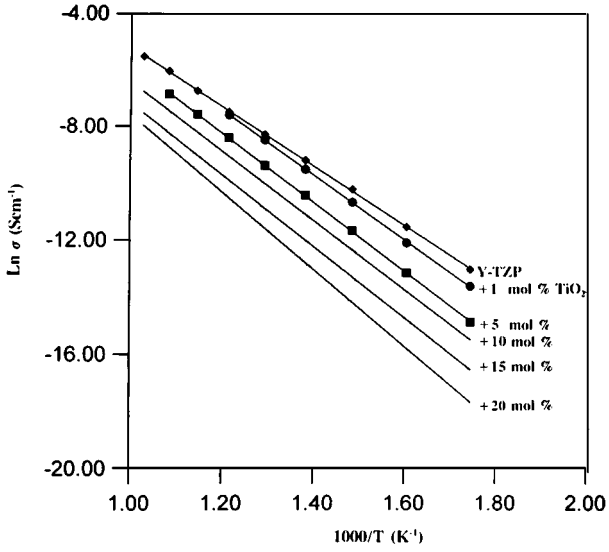

Figure 5 Temperature dependence of the total conductivity in $(TiO_2)_x$-(Y-TZP)$_{1-x}$ tetragonal zirconia solid solutions.

content as shown in Fig. 5, can be observed, and from Table III the similar activation energy value for the bulk and the total conductivity processes allows one to assume that a bulk oxygen ions transport seems to be predominant in the samples studied.

4. Discussion

From the XRD lattice parameter measurements, (see Fig. 1), it can be stated that the solubility limit for titania in yttria stabilized tetragonal zirconia up to 1400 °C is close to ∼13 mol %. Compositions containing higher titania content showed the incipient presence of a second phase, the zirconium titanate (ZT), and for higher yttria content appeared the zirconia phase with cubic structure in agreement with that established for ZrO_2-Y_2O_3 binary system [32, 33].

It was also noticed that the tetragonality, c/a, of the zirconia solid solutions increases with increasing content of the TiO_2 dopant, see Fig. 1, and this became constant for a TiO_2 content near to 14 mol % confirming the above statement for the solubility limit of TiO_2 in yttria stabilized tetragonal zirconia, Y-TZP, in close agreement with the results of Lin *et al*. [34]. This solid solution with a tetragonality of about 1.024 much higher than that of the binary tetragonal zirconia-yttria solid solution [33], 1.016, is also stable at room temperature. Albeit the stability of the tetragonal zirconia solid solution needs the creation of oxygen vacancies, and the addition of Ti^{4+} implies a dilution effect with a slight decreasing of the oxygen vacancy concentration, then the enhanced stability of the ternary tetragonal zirconia solid solutions can be explained by two coadjutant effects, (i) The presence of a relatively high concentration of oxygen vacancies introduced by Y^{3+} dopant and (ii) Albeit the Ti dopant could decrease the stability of the Y-stabilized tetragonal zirconia by diluting the effect of the oxygen vacancies introduced by Y^{3+}, but the measured Ti-O distances (1.88 Å), being shorter than the Zr-O_I distances (2.10 Å) leads to an accentuated bonding anisotropy of the layer-like zirconia structure and, therefore, to a higher tetragonality. Besides this, the size of the Ti^{4+} cation ($RTi^{4+} = 0.745$ Å) which is much smaller than Zr^{4+} ($RZr^{4+} = 0.86$ Å), adopting a five-fold coordination would favor a packing in the form of a relatively ordered layer-like structure alleviating, thus, the oxygen overcrowding around Zr cations similarly to that occurring in the GeO_2-doped tetragonal zirconia [23].

Ordering involving the smallest Ti cations was not demonstrated in the case of the titania-doped YTZP solid solutions, but a Ti cationic short-range ordering was detected by TEM in the ZrO_2-CeO_2-TiO_2 system for a stable composition having a tetragonality as high as 1.032 [35]. The Ti-Ti distances measured here (2.81 Å) much shorter than 3.62 Å for Zr-Zr ones, allows us to assume a certain Ti cationic ordering sufficient to reduce the strain energy of the tetragonal lattice leading to a higher stability of the titania-doped tetragonal zirconia solid solutions.

Fourier transforms (FTs) of the Ti EXAFS for tetragonal 5Ti-YTZP and 10Ti-YTZP, as pseudoradial distribution functions of the absorber atom, can be used to compare structures surrounding Ti cation, see Fig. 2. From those results, it can be stated a non randomly substitutional model when dissolving TiO_2 into yttria-doped tetragonal zirconia. The ternary Ti-YTZP solid solution becomes more distorted with increasing TiO_2 content. Such an increasing distortion indicates a change in the coordination number of the Ti cations with the subsequent loss of centrosymmetry in the crystal lattice of the tetragonal zirconia. Such a statement is supported by the increase of the intensity of the pre-edge peak and the decrease in energy of the post-edge peak with increasing TiO_2 content, as shown in the XANES spectra (Fig. 2a).

From the EXAFS spectra analysis for the 5Ti-YTZP sample it must be noticed a Ti-O distance of 1.73 Å, which is comparable to that corresponding to Ti^{4+} cations tetrahedrally coordinated as in the case of the compounds Ba_2TiO_4 (1.74 Å) and $Ti(OAm)_4$ (1.81 Å), but the total coordination number for the 5Ti-YTZP sample was near to 6. This result leads to assume that, similarly to that occurring in TiO_2-SiO_2 glasses, [28] when the TiO_2 concentration was low the Ti^{4+} prefer the octahedral coordination in the glass network, and for higher concentration the Ti^{4+} adopts the five-fold coordination. A similar phenomenon seems to be present in the Ti-YTZP solid solutions with increasing TiO_2 content. Such a coordination change leads to assume a strong distortion of the tetragonal zirconia lattice, albeit the measured Debye-Waller factors, see Table II, being positive, are relatively small to support a very severe tetragonal zirconia lattice distortion. Therefore with the present EXAFS and XANES data it can be said that the Ti^{4+} cations in the Ti-YTZP solid solutions are displaced from the center of the coordination polyhedron adopting a non octahedral coordination,

presumably five-fold coordinated in a square-pyramidal arrangement. In our opinion, an exhaustive study of these Ti-YTZP ternary solid solutions which including the EXAFS spectra at the Zr-K and Y-K edges would contribute to a better knowledge of the crystal chemistry of Ti^{4+} in these zirconia solid solutions. It will form the objective of a subsequent work.

Finally, the shorter Ti-O distances favoring a movement to an off center position, and the Ti-Ti measured distances lead to assume a strong interaction between the Ti cations with a certain tendency to the formation of clusters. Such a clustering phenomenon can provoke a different oxygen ions bonding in the tetragonal zirconia lattice and, of course, a different bond strength of the oxygen vacancies associated with both Zr^{4+} or Ti^{4+} cations having different coordination numbers.

The electrical behavior of TiO_2-doped zirconia solid solutions, mainly in the cubic structure, has been widely studied [6–9]. However, none of them explained the true role of the crystal chemistry of the Ti ions in the TiO_2-cubic zirconia solid solutions. Recently Traqueia *et al*., [36] making use of the Raman spectroscopy, tried to correlate the electrical conductivity decrease with increasing titania content in TiO_2-doped cubic zirconia with the presence of a tetragonal short range order in the cubic zirconia matrix. Such a short range order decreased the concentration of the mobile oxygen vacancies and, thus, the electrical conductivity also was decreased.

The present results on the electrical conductivity in air TiO_2-doped tetragonal zirconia solid solutions show the same dependence, as shown by Arashi and Naito [8] i.e., the electrical conductivity in air decreases with increasing titania content. Such a behavior can be explained on the basis of the study of the Ti ions local environment from the EXAFS and XANES spectra data, see Figs 2 and 3. From those results and taking into account the Li *et al*. [37] model, it is assumed that the oversized Y^{3+} cations substitute for Zr^{4+} in the cation network adopting a YO_8 structure and, therefore, Y^{3+} will not be associated with oxygen vacancies. Being this so, then those eightfold dopant coordination leaves oxygen vacancies near to the both Zr and Ti cations, since the Zr(Ti)-vacancy pairing is energetically more favorable than Y-vacancy pairing in Y-doped zirconia as previously suggested [37]. In that situation, an undersized tetravalent dopants as the Ti^{4+} cations, which do not substitute randomly for Zr ions in tetragonal zirconia solid solutions, and by adopting a five fold coordination with a square based pyramidal arrangement are, thus, in competition with Zr ions for the oxygen vacancies. On that basis, two kind of vacancy (Vö)-cation associations have to be formed, one of them Zr-Vö in which the oxygen vacancy is associated to a cation octahedrally coordinated, and the other one Ti-Vö with oxygen vacancy associated to a cation fivefold coordinated according to the following reactions:

$$Y_2O_3(TiO_2) \xrightarrow{ZrO_2} Y'_{Zr} + Ti'_{Zr} + Vö + 5O^x_o$$

$$Ti'_{Zr} + Vö \longrightarrow Ti'_{Zr}Vö$$

$$Zr_{Zr} + Vö \longrightarrow Zr_{Zr}Vö$$

With such a statement it must be also assumed two oxygen sublattice with different vacancy diffusion dynamics. Given that the Ti-O distances are shorter that the Zr-O ones, we state that the oxygen vacancy diffusion on the octahedrally coordinated sublattice is more rapid than on the square based pyramidal fivefold sublattice, and a hindering (trapping) for the mobility of the oxygen vacancies is produced, thus, by the presence of the Ti ions in the TiO_2-doped tetragonal zirconia solid solutions. This is supported by the fact that the activation energy for the conduction process is higher in TiO_2-doped YTZP than in undoped-YTZP, see Table III. On the other hand, the shorter Ti-Ti measured distances will show a certain tendency to the formation of Ti clusters and thus, to an increasing degree of the oxygen vacancy-titanium cation complex associations that, in the case of the formation of the simplest cluster, i.e., two titanium atoms, the more complex oxygen vacancy-Ti^{4+} cation would be formed as follows,

$$Ti'_{Zr}Vö + Ti'_{Zr} + Vö \rightarrow Ti'_{Zr}VöTi'_{Zr}Vö$$

these structural "dimers," should be homogeneously distributed in the tetragonal zirconia lattice.

All these assumptions, based on the Ti EXAFS and XANES data and assuming the Li *et al*. [37] defects model, would implies the non existence of associates (Y'_{Zr} Vö) in the zirconia lattice, which is in contradiction with the interpretation of ionic conductivity in Y-TZP (3 mol % Y_2O_3) by Weller *et al*. [38, 39]. They assumed the formation of Y'_{Zr} Vö complexes which are oriented parallel to [1 1 1] directions in tetragonal zirconia polycrystals Y-TZP and, accordingly, it could be expected that Y'_{Zr} and Vö ions would be arranged on nearest-neighbor positions. Given that the (Y'_{Zr} Vö) complexes can be considered as anisotropic elastic and dielectric dipoles that are able to be reoriented upon application of elastic or electric fields causing, thus, mechanical or electrical loss, then, it was also assumed that the mechanical and dielectric losses produced during the reorientation of such (Y'_{Zr} Vö) dipoles took place by the jumping of the oxygen vacancies around the Y'_{Zr} ions. Furthermore, the similarity of the activation enthalpies for both the mechanical and dielectric relaxation processes and the low-temperature ionic conductivity in Y-TZP enabled them to conclude that these are controlled by the jumping of oxygen vacancies around the yttrium atoms. In the case of the present Ti-YTZP solid solutions, having a tetragonality $c/a \simeq 1.024$, much higher than that of Y-TZP ($\approx$1.016), the relaxation jump of oxygen vacancies along the *a*-axis or the *c*-axis will occurs with slightly different frequencies because of the different distances of neighboring oxygen sites between the two axes directions. By assuming that the different defect complexes as (Zr Vö), (Ti'_{Zr} Vö) and or (Ti'_{Zr} Vö Ti'_{Zr} Vö) may be the cause for the different type of relaxation, as well as that the Zr Vö and Ti'_{Zr} Vö cation-vacancy interaction can give rise to the distribution of relaxation time and enthalpy for relaxations, then the internal friction has to be attributed to point defects and these are either Zr and Ti ions and oxygen ion vacancies. If the activation energy for internal friction is close to that for oxygen vacancies migration [39],

then the internal friction has to be attributed to those point defects and not to others. Therefore, a better understanding of defect properties in tetragonal zirconia ceramics should be carried out in the future. For example, a deep knowledge of the relaxation behavior and the conductivity relationship and the enthalpies for both processes, becomes necessary to know the true type of defects present in the Ti-YTZP solid solutions.

Acknowledgement

The authors wish to thank Dr. R. Rojas for fruitful discussion, and Spanish Commission of Science and Technology (CICYT) supporting under the contract MAT 97-0679-Co2-01.

References

1. N. A. MINH, *J. Am. Ceram. Soc.* **76** (1993) 563.
2. R. FULLMAN and S. P. MITOFF, U.S. Paten No 3.410, (1968) 728.
3. B. CALES and J. F. BAUMARD, *J. Electrochem. Soc.* **131** (1984) 2407.
4. S. S. LIOU and W. L. WORRELL, *Appl. Phys. A* **49** (1989) 25.
5. K. E. SWIDER and W. L. WORRELL in "Solid Oxide Fuel Cells," edited by S. C. Singhal (Electrochem. Soc. Second Int. Symp. Rec., Pennington, N.J., 1991) p. 593.
6. S. S. LIOU and W. L. WORRELL, Proc. 1st. Int. Symp. on Solid Oxide Fuell Cells, edited by S. C. Singhal (The Electrochemical Society, Pennington, 1989) p. 81.
7. P. V. ANANTHAPADNEMABHAN, N. VENKATRAMANI, V. K. ROHATGI, A. C. MOMIN and K. S. VENKATESWARLU, *J. Europ. Ceran. Soc.* **6** (1990) 111.
8. H. ARASHI and H. NAITO, *Solid State Ionics* **53–56** (1992) 431.
9. H. NAITO and H. ARASHI, *ibid.* **53–56** (1992) 436.
10. A. KORR, H. NAFE, W. WEPPNER, P. KONTOUROS and H. SCHUBERT, "Science and Technology of Zirconia V," edited by S. P. S. Badwals *et al.* (Technomic, Lancaster, PA, 1993) p. 567.
11. G. ROG and G. BORCHARDT, *Ceramics Inrern.* **22** (1996) 149.
12. A. S. NOWICK, "Diffusion in Crystalline Solids," edited by G. E. Murch and A. S. Nowick (Academic Press, Orlando, FL, 1984) chap. 3.
13. F. CAPEL, PhD thesis, Complutense University of Madrid, 1998.
14. B. K. TEO, "EXAFS: Basic Principles and Data Analysis" (Springer-Verlag, New York 1986).
15. R. A. SCOTT, *Methods Enzymol* **177** (1985) 414.
16. D. BONIN, P. KAISER, C. FREGNY and J. DESBARRES, "Structures Fines D'absorption en Chimie," edited by H. Dexpert *et al*. (Orsay, 1989).
17. J. J. REHR, J. M. de LEON, S. J. ZABINSKY and R. C. ALBERS, *J. Am. Chem. Soc.* **113** (1991) 5135.
18. F. CAPEL, C. MOURE, P. DURÁN and M. A. BAÑARES, *Mater. Lett*. **38** (1999) 331.
19. H. HOFFMAN, B. MICHEL and L. J. GAUCKLER, "Advances in Zirconia Science and Technology-Zirconia' 88," edited by S. Meriani and C. Palmonari (Elsevier Applied Sciences, 1989) p. 119.
20. C. J. HOWARD, B. A. HUNTER and D. J. KIM, *J. Am. Ceram. Soc.* **24** (1998).
21. D. MICHEL, M. T. VAN den BORRE and A. ENNACIRI in "Advances in Ceramics," Vol. 24 A, edited by S. Somiya, N. Yamamato and H. Yanagida (The Am. Ceram. Soc., Columbus, OH 1989) p. 555.
22. P. LI, I. W. CHEN and J. E. PENNER-HAHN, *J. Am. Ceram. Soc*. **77** (1994) 1281.
23. *Idem*., *Phys. Rev. B* **48** (1993) 10074.
24. R. C. CATLOW, A. V. CHADWICK, G. N. GREAVES and L. M. MORONEY, *J. Am. Ceram. Soc*. **69** (1986) 272.
25. E. ZSCHECH, P. N. KONTOUROS, G. PETZOW, P. BEHRENS, A. LESSMANN and R. FRAHM, *ibid*. **76** (1993) 197.
26. G. A. WAYCHUNAS, *Am. Mineral*. **72** (1987) 89.
27. T. DUMAS and J. PETIAU, *J. Non-Cryst. Solids* **81** (1986) 201.
28. C. A. YARKER, P. A. V. JOHNSON, A. C. WRIGHT, J. WONG, R. B. GREEGOR, F. W. LYLE and R. N. SINCLAIR, *ibid*. **79** (1986) 117.
29. J. LIVAGE, "Chemical Processing of Ceramics," Vol. 3 (Marcel-Derker, Inc., New York, 1944).
30. M. J. VERKERK, B. J. MIDDELHUIS and A. J. BURGGRAAF, *Solid State Ionics* **6** (1982) 159.
31. J. A. KILNER and B. C. H. STEELE, "Nonstoichiometric oxides," edited by D. T. Sorensen (Academic Press, Inc., New York, 1981) p. 233.
32. C. PASCUAL and P. DURAN, *J. Am. Ceram. Soc*. **66** (1983) 23.
33. H. G. SCOTT, *J. Mater. Sci*. **10** (1975) 1527.
34. C. L. LIN, D. GAN and P. SHEN, *Mater. Sci. and Engineering A* **129** (1990) 147.
35. V. C. PANDOLFELLI, W. M. RAINFORTH and R. STEVENS, in "Proc. of 1st Europ. Ceram. Soc. Conf," edited by G. Dewith *et al*. (Elsevier Science Publishing, New York, 1989) p. 161.
36. L. S. M. TRAQUEIA, T. PAGNIER and F. M. B. MARQUES, *J. Europ. Ceram. Soc*. **17** (1997) 1019.
37. P. LI, I. W. CHEN and J. A. PENNER-HAHN, *J. Am. Ceram. Soc*. **77** (1994) 118.
38. M. WELLER and H. SCHUBERT, *ibid*. **69** (1986) 537.
39. M. WELLER, H. SCHUBERT and P. KONTOUROS, "Science and Technology of Zirconia V," edited by S. P. S. Badwal *et al*. (Technomic, Lancaster, PA, 1993) p. 546.

Received 9 November 1998
and accepted 15 July 1999